

# Initial results of the Geosynchronous Synthetic Thinned Array Radiometer (GeoSTAR)

Alan B. Tanner, W.J.Wilson, B.H.Lambrigsten,  
S.J.Dinardo, S.T.Brown, P.Kangaslahti, and  
T.C.Gaier

Jet Propulsion Laboratory  
California Institute of Technology  
Pasadena, USA  
Alan.b.tanner@jpl.nasa.gov

C.S.Ruf, S.M.Gross, B.H.Lim, S.Musko, and S.  
Rogacki

University of Michigan  
Ann Arbor, MI

**Abstract**—The design and preliminary test results of a 50-56 GHz synthetic aperture radiometer demonstration system are discussed. An error budget is presented to meet 1 Kelvin radiometric accuracy in a geostationary atmospheric sounder with 50 km spatial resolution on the earth. The gain and phase errors are weighted by the magnitude of visibility versus antenna separation, and requirements range between ~0.5% and 0.3 degrees of amplitude and phase, respectively, for the closest spacings at the center of the array, and about 5% and 3 degrees for the majority of the array. The latter requirement is met by our design without any special testing or stabilizations by reference signals. The former is met using an internal noise diode reference and by measuring the detailed antenna patterns on the antenna range. Biases and other additive errors in the raw visibility samples must be below about 2 mK on average, and this requirement is met by a phase shifting scheme applied to the local oscillator distribution. An outline of the data processing is presented, along with the first images from this system.

**Keywords**— remote sensing; radiometer; interferometer.

## I. INTRODUCTION

GeoSTAR is a concept to provide high spatial resolution soundings of the earth's atmosphere from geosynchronous orbit (GEO) in microwave bands from 50 GHz to 180 GHz [1]. 2-D images are synthesized by Fourier Transform of interferometric data collected with a Y-array of correlation interferometers. The concept eliminates the need for large mechanically scanned apertures, but it poses many new challenges--particularly in the area of calibration. This paper presents preliminary results of a small (24-element) 50-56 GHz system which has been built under NASA's Instrument Incubator Program to demonstrate the basic technology and calibration techniques needed for a large (300 element) system.

## II. INSTRUMENT CONCEPT AND ERROR BUDGET

GeoSTAR consists of a Y-array of receivers configured in the geometry of Figures 1 and 2. The antennas share the same field of view (FOV) and the IF signals of all receivers are simultaneously cross-correlated against one another in a digital subsystem. Each correlated antenna pair forms an interferometer which measures a particular spatial harmonic of

the brightness temperature across the FOV. When expressed as a function of antenna spacing-- or "baselines" with dimensions "U" and "V" by astronomy convention-- this complex cross-correlation is called the visibility function. The visibility function is the Fourier transform of the brightness temperature image. With sufficient sampling over a range of spacings one can reconstruct, or synthesize, a 2-D image by inverse transform. The "Y" configuration provides these samples using a minimum number of antennas and with a fixed geometry-- in a so called thinned array. As illustrated in Fig. 1, the spacings between the various antenna pairs yield a uniform hexagonal grid of visibility samples in the UV plane. There are 8 elements in each arm of Fig. 1, and this yields 64 unique spacings between arms 1 and 2, for example. Another 64 conjugate-symmetric samples are derived by subtracting arm 2 from arm 1. In all, the 24-element system produces 384 UV samples (=6\*64). Note, in this particular layout, that all of the UV samples are formed between elements in different arms, and that none are necessarily formed between elements within an arm. This scheme simplifies the electrical and mechanical design, as detailed in Section III.

The smallest spacing of the sample grid in Fig. 1 determines the unambiguous field of view (FOV), which for GeoSTAR must match the earth disk diameter of 17.5° when viewed from GEO. This sets both the antenna element spacing and diameter at about 3.75 wavelengths, or 2.25 cm at 50 GHz. The longest spacing determines the smallest spatial scale that can be resolved. The synthetic aperture diameter of Fig. 1 is 60 cm, which yields about 0.6 degrees of angular resolution for the demonstrator system. 50 km spatial resolution on the earth will require 100 receiving elements per array arm in a GEO system. This will produce 60,000 UV samples and 60,000 linearly independent image pixels within the FOV.

Our design is based on an overall calibration requirement of 1 Kelvin error in the synthesized brightness temperature image of the earth. This translates into error allocations for individual visibility samples. Our analysis divides errors into categories of either "gain" or of "additive" errors. Gain errors include anything that results in an uncertain amplitude scaling or phase shift in the visibility measurements. These include uncertainties in elemental antenna patterns and array alignment, as well as uncertainties of the gain and phase response of the correlators. The simplest analysis allocates these errors equally

---

This work has been carried out at the Jet Propulsion Laboratory, California Institute of Technology under a contract with the National Aeronautics and Space Administration.

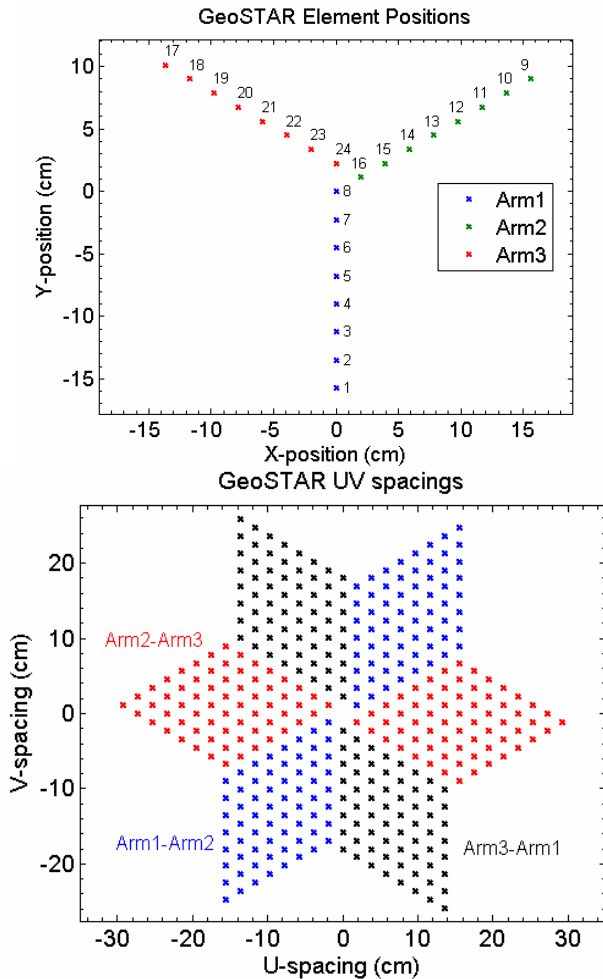


**Fig. 1.** Antenna array layout (above) and corresponding UV samples of the synthetic aperture (below). Each UV sample is a difference between XY positions of two antennas (i.e. for antennas A and B  $u_{AB}=X_A-X_B$ ,  $v_{AB}=Y_A-Y_B$ ).

to all visibility samples. In this case gain errors must simply be a small fraction of the nominal brightness of the earth-- or roughly 0.3% to keep errors below 1K out of a mean temperature of 300 K. A better analysis allocates errors according to the magnitude of the expected visibility. Only the zero-baseline-- which measures the mean temperature of the scene-- has a magnitude approaching 300 K. This sample is actually measured with a conventional Dicke radiometer (not shown in Fig. 1 or 2). All of the non-zero baselines-- namely all of the correlated pairs-- have much smaller magnitudes, and requirements can be relaxed accordingly. Based on models of the earth brightness, visibility magnitudes are at most ~20 Kelvin near the center of the UV plane, and otherwise less than ~0.1 Kelvin in the great majority of UV samples. This allows for gain and phase errors of ~ 5 percent and ~ 3 degrees, respectively, in most correlators. Only those elements near the center of the array need to be calibrated to precisions approaching ~0.5 % in gain and 0.3 degrees of phase.

Additive errors include correlator biases (null offsets) and the basic measurement noise set by system noise, bandwidth, and integration time. These errors add directly to the image such that one Kelvin error added to any one visibility will add 1 Kelvin RMS error to the image. If such errors are uniform

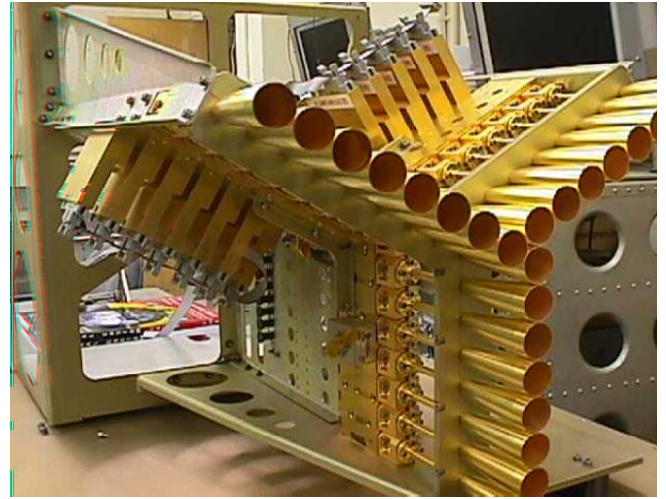


**Fig 2.** GeoSTAR demonstrator instrument

through the array, then image errors increase as  $\text{SQRT}(N)$ , where  $N$  is the number of visibility samples in the Fourier Series. This imposes a requirement that becomes stricter as the array size increases. With  $N=60,000$  UV samples, the RMS visibility errors must be less than about 2 mK ( $=0.5 \text{ K} / \text{SQRT}(60,000)$ ). Note that this requirement changes with  $N$ , whereas gain requirements are largely invariant with  $N$ .

### III. DEMONSTRATOR INSTRUMENT

The GeoSTAR demonstrator instrument operates at 4 AMSU channels between 50 and 56 GHz. A simplified block diagram is given in Fig. 3. From left to right in Fig. 3 (or from front to back in Fig. 2) the signal starts at the horn apertures with horizontal polarization. The horns are a variant of a Potter horn which adds a parabolic profile section to broaden the useful RF band to 50-56 GHz. This design permits very close spacing in the array while maximizing the aperture area. This is important for the GEO observation as it maximizes the fraction of the antenna energy which is received from the earth disk. This fraction is about 50% with this design. The aperture taper reduces mutual coupling and array embedding effects, which simplifies the antenna modeling problem. The reduction of coupling between antennas is also crucial for controlling correlation biases caused by the leakage of receiver noise from one antenna to another. Ferrite isolators (not shown in the diagram) are added to the six closest elements at the center of the array to further suppress these biases where the coupling is greatest (about -60 dB between adjacent elements). Continuing in Fig. 3, each horn incorporates a circular to rectangular transition followed by a waveguide twist of either 0, +60, or -60 degrees to match the orientation to the three arms in Fig. 2. These twists provide a simple and precise polarization alignment. We considered circular polarizers, but found they were not easily balanced through the 10% bandwidth.

The signal in Fig. 3 next passes through an 8-way calibration feed manifold which periodically injects a noise signal into all receivers from a common noise diode source. This signal provides a reference to stabilize the system against gain, phase, and receiver noise drifts. The injected signal

reaches the receiver inputs with about 5 K equivalent noise temperature. The noise diode signal is distributed to the three arms via phase shifters. These were intended as a means to resolve the quadrature balance of each correlator, but later proved redundant with other circuits described below. Next, the antenna signal passes into the MMIC receiver module where it is amplified using InP FET low noise amplifiers and then double-sideband downconverted by subharmonic quadrature mixers to two IF baseband signals. Receiver noise is about 400 K. Each receiver also contains a programmable bias circuit which can adjust the gate and drain voltages of each amplifier stage to affect gain and noise figure. This circuit was originally envisioned as calibration tool (e.g. to switch off a receiver and thereby measure correlator biases), but it has proved more useful to balance and tune the receivers during production and tests. The local oscillator of Fig. 3 operates from 25 to 28 GHz to tune from 50 to 56 GHz at RF. The LO is distributed via three 2-bit phase shifters. These periodically shift the phase to each arm by 45, 90, or 135 degrees, which results in shifts of 90, 180, and 270 degrees, respectively at RF. As discussed in Section IV, this circuit proved superior to the above noise diode phase shifters and to the amplifier controls when estimating quadrature balance and correlator biases.

The in-phase (I) and quadrature (Q) IF signals from each mixer are next amplified and filtered to define the passband. These signals are then digitized at a clock rate of 220 MHz. For reasons of product availability the analog to digital converter is presently an 8-bit device, but this could be replaced with a one-bit converter. The correlators only use 1-bit (the sign bit). One-bit correlators require the least power with a relatively minor penalty in sensitivity, which is a fair tradeoff given the great number of correlators required by GeoSTAR. The correlator of Fig. 3 is implemented in an FPGA.

#### IV. DATA PROCESSING AND EARLY TEST RESULTS

The 1-bit correlations are first mapped to linear correlations using the Van Vleck formula [2]. This removes the nonlinearity of a 1-bit correlator when the input signals are known to be Gaussian. This step is applied to all four

correlators associated with each antenna pair. Each antenna is associated with an “I” and a “Q” IF signal, so each antenna pair is associated with four correlators: “II”, “QQ”, “QI” and “IQ”. This represents a two-fold redundancy in our data which we use to reduce measurement noise. If there were no biases, and if the subharmonic mixers of Fig. 3 were perfectly balanced in quadrature, then these four correlations could be immediately combined into a single complex correlation. Yet the quadrature balance is known to be poor-- on the order of 10 degrees of phase-- and the raw correlations are known to contain large biases due to digitizer null offsets and leakage of correlated noise from the LO. To fix this, the LO phases are shifted in a sequence that rotates all correlations to all four phase quadrants. The exact phase shifts are determined from network analyzer measurements made prior to system integration. These are applied in a linear regression to resolve the amplitude, offset, and phase of each correlator. This yields four complex correlations which are redundant in their expected values, but independent in noise. These are averaged to form the final complex correlation. This process ensures very precise quadrature balance, and virtually eliminates biases caused by anything other than direct leakage of the RF signals among the antennas. At present, we have observed total biases ranging from about 3 mK in the larger baselines to 40 mK in the short baselines, due almost entirely to leakage between antennas. This nearly meets our 2 mK goal in all but a small fraction of UV samples. The remaining biases are stable, and should be easily corrected.

The above correlations are next scaled to visibility using an estimate of the system noise temperature, and then aligned in phase to the aperture plane. We have thus far used LN2 and ambient targets to estimate receiver noise temperature, and point sources on an antenna range to align the phase. These references are transferred to operations by at least two methods: the first uses the internal noise diode to deflect the correlation and system noise by a reliable amplitude and phase. This provides a convenient and steady reference, but there are noise penalties due to the time required to measure the noise diode. The second method relies on the intrinsic stability of the receivers. The receiver noise temperatures of GeoSTAR are quite stable at the ~2K level, which represents about 0.3% of

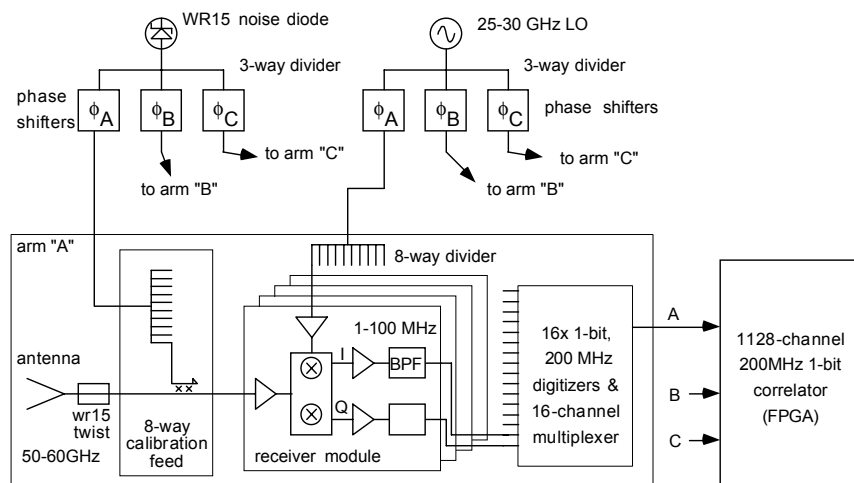
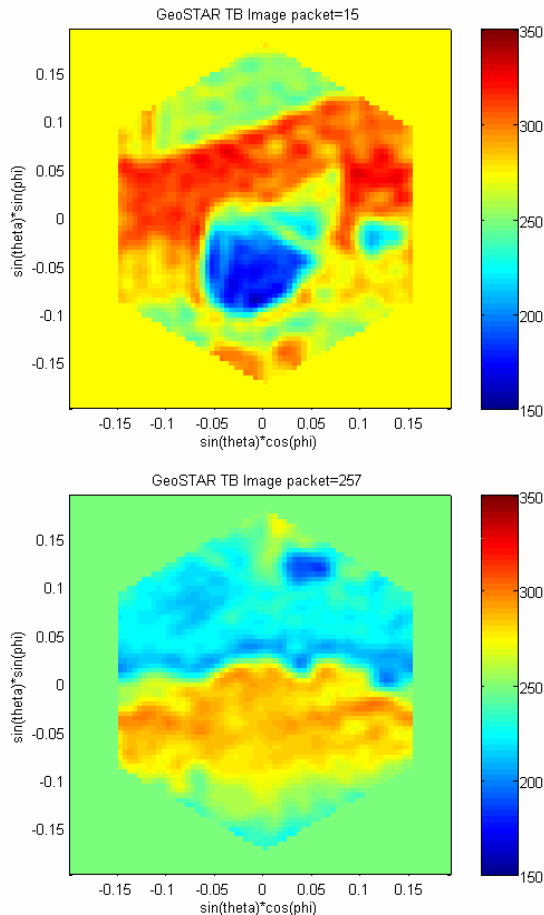
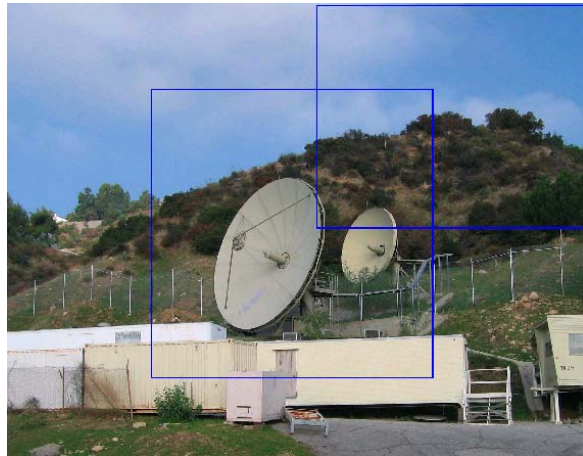


Fig 3. Receiver system block diagram – one of three arms shown

the  $\sim 700$  K system noise. The observed phase stability is better than  $\sim 1$  degree. These stabilities readily satisfy the phase and amplitude needs of most correlators. To meet the stricter phase requirements for correlations near the center of the UV plane, we will likely need the noise injection. This is an ongoing study, but we now envision a hybrid scheme in which uses long running averages of low duty cycle noise diode injection--possibly applied only to those correlators near the center of the UV plane.



**Fig 4.** GeoSTAR images of hillside at 50.3 GHz with reference photograph and approximate frame positions.

The visibilities are next transformed into an image. Ideally, this step is a Fourier Transform followed by a scaling within the earth disk by the elemental antenna pattern. This requires, among other things, that the pattern of every antenna element be identical and precisely characterized by a single model. Our goal is to come as close as possible to this ideal-- to within 0.5% in the short baselines and 5% in the longer baselines. We have recently performed end-to-end system tests on the antenna range which validate our model at the 2% level, and show consistency among antenna elements at the 1% level. We have also used solar observations to validate the antenna range results at the 0.5% level. Details are beyond the scope of this paper, but these are very encouraging results which clears a path to a workable calibration. We envision a G-matrix solution [3] for short baselines, based on precise antenna measurements, and a Fast Fourier Transform for the larger baselines where requirements are relaxed.

Fig. 4 presents the first images from GeoSTAR, as measured November 2, 2005 looking towards the hills north of JPL. These were produced with a straight Fourier Transform, without any corrections for elemental patterns or for biases from mutual coupling. In spite of these errors, the quality is quite good. The large dish antenna and the horizon boundaries are clearly visible and geometrically accurate. The hexagonal image boundary represents our unambiguous FOV, which represents a single period of the Fourier integral given the hexagonally gridded UV samples of Fig. 1. Beyond this region, the Fourier Series replicates the same hexagonal image (with the same orientation). We refer to these as the aliased regions. These regions are largely suppressed by the elemental pattern, but the residual sensitivity does affect the main image. In space, these regions will be off of the earth disk, and do not pose a problem. In the present images, the aliased regions result in some artifacts: note that in the image of the hillside that there is an anomalously cold region in the sky to the upper right; this can be traced to aliasing from the small dish antennas which is just outside of the image to the lower left (visible in the photograph). These effects are well understood, and do not pose a problem for the GEO application.

#### ACKNOWLEDGMENT

This work has been carried out at the Jet Propulsion Laboratory, California Institute of Technology under a contract with the National Aeronautics and Space Administration.

#### REFERENCES

- [1] B. Lambrigtsen, W. Wilson, A. Tanner, T. Gaier, C. Ruf, J. Piepmeier, "GeoSTAR - a microwave sounder for geostationary satellites", IEEE Proceedings IGARSS '04, Vol. 2, pp. 777 - 780, 2004.
- [2] Thompson, A.R., Moran, J.M., Swenson, G.W., Jr., Interferometry and Synthesis in Radio Astronomy, Wiley-Interscience, 1986
- [3] Tanner, A.B., and Swift C.T., "Calibration of a Synthetic Aperture Radiometer," IEEE Trans. Geoscience & Remote Sensing, Vol.31, No. 1, Jan. 1993.